

CHEMISTRY OF MATERIALS

VOLUME 19, NUMBER 23

NOVEMBER 13, 2007

© Copyright 2007 by the American Chemical Society

Articles

Controlled Scalable Synthesis of ZnO Nanoparticles

Karel J. Hartlieb,^{†,‡} Colin L. Raston,^{*,†} and Martin Saunders[‡]

Centre for Strategic Nano-Fabrication, School of Biomedical, Biomolecular and Chemical Sciences, and
Centre for Microscopy, Characterisation and Analysis, The University of Western Australia,
35 Stirling Highway, Crawley WA 6009, Australia

Received June 11, 2007. Revised Manuscript Received August 24, 2007

Zinc oxide nanoparticles are formed under continuous flow using spinning disc processing (SDP). Synthetic parameters such as temperature, flow rate, disc speed, and surface texture influence the reaction kinetics and particle size in an ethanolic solution using polyvinylpyrrolidone (PVP) as a capping agent. SDP ensures intense mixing, accelerates nucleation and growth, and affords monodispersed ZnO nanoparticles with controlled particle size. UV–visible spectroscopy shows the formation of particles down to a size of 1.3 nm and polydispersities of approximately 10%, as well as subnanometer clusters. Modification of the temperature and flow rate provides control of the particle size and polydispersity, albeit with the nanoparticles slowly undergoing ripening post-SDP.

Introduction

The synthesis of semiconducting nanoparticles has generated a considerable amount of interest in the past few decades because of the interesting size-dependent optical and electronic properties they display and, consequently, their potential in many applications. Zinc oxide, which has a bulk, direct band gap of 3.3 eV at room temperature with a free exciton binding energy of 60 meV,¹ displays piezoelectric

properties² and is one of the many technologically important semiconducting materials with a variety of applications, including chemical sensors,³ catalysts,^{4,5} UV light-emitters,^{2,6,7} phosphors,⁸ photovoltaics,^{9,10} cantilevers,¹¹ varistors,¹²

- (2) Cho, S.; Ma, J.; Kim, Y.; Sun, Y.; Wong, G. K. L.; Ketterson, J. B. *Appl. Phys. Lett.* **1999**, *75*, 2761–2763.
- (3) Tamaki, J. *Sens. Lett.* **2005**, *3*, 89–98.
- (4) Kurtz, M.; Strunk, J.; Hinrichsen, O.; Muhler, M.; Fink, K.; Meyer, B.; Wöll, C. *Angew. Chem., Int. Ed.* **2005**, *44*, 2790–2794.
- (5) Sarvari-Hosseini, M.; Sharghi, H. *J. Org. Chem.* **2006**, *71*, 6652–6654.
- (6) Yang, C. L.; Wang, J. N.; Ge, W. K.; Guo, L.; Yang, S. H.; Shen, D. *Z. J. Appl. Phys.* **2001**, *90*, 4489–4493.
- (7) Cao, B.; Li, Y.; Duan, G.; Cai, W. *Cryst. Growth Des.* **2006**, *6*, 1091–1095.
- (8) Li, Y. Y.; Li, Y. X.; Wu, Y. L.; Sun, W. L. *J. Lumin.* **2007**, *126*, 177–181.
- (9) Law, M.; Greene, L. E.; Johnson, J. C.; Saykally, R.; Yang, P. *Nat. Mater.* **2005**, *4*, 455–459.

* Corresponding author. E-mail: clraston@chem.uwa.edu.au. Phone: 61 86488 3045. Fax: 61 86488 8683.

[†] Centre for Strategic Nano-Fabrication, The University of Western Australia.

[‡] Centre for Microscopy, Characterisation and Analysis, The University of Western Australia.

(1) Polarz, S.; Roy, A.; Merz, M.; Halm, S.; Schröder, D.; Schneider, L.; Bacher, G.; Kruis, F. E.; Driess, M. *Small* **2005**, *1*, 540–552.

and other optoelectronic devices.¹³ In addition, ZnO is nontoxic, at least in the bulk form, relatively cheap, and stable in air. Many different synthesis routes for the production of ZnO nanoparticles with various morphologies have been established, including sol-gel,^{14,15} wet chemical synthesis,^{16–23} and gas-phase techniques such as chemical vapor deposition^{1,24} and spray pyrolysis.^{25–27} A large number of the reported techniques involve elaborate, time-consuming steps, long reaction times, and/or the use of toxic precursors. To exploit the size-dependent properties such materials exhibit, it is important to be able to prepare nanomaterials with a controlled size and size distribution on a commercial scale, ideally under continuous flow. One of the most significant issues hindering the commercial production of nanomaterials is scalability and although many thousands of papers have been published with regards to the synthesis and applications of nanomaterials, products containing nanomaterials make up only a small fraction of the current market. An additional factor that must be addressed is the environmental impact of the chemical synthesis of nanomaterials, and therefore, a sustainable approach to commercial production must be considered.²⁸

Here, we report the synthesis of ZnO nanoparticles using a process intensification strategy known as spinning disc processing (SDP) technology. SDP makes use of centrifugal acceleration to create very thin films of fluid (1 to 200 μm) on a surface by supplying solutions to the surface of a rapidly rotating disc (300–3000 rpm), thus creating conditions of high mass and heat transfer, Figure 1. High shear forces generated in the thin fluid films produce waves that intensify mixing of the fluid. This means that all reactants are subjected to exactly the same conditions, unlike conventional batch reactors. There are no difficulties in scale-up for

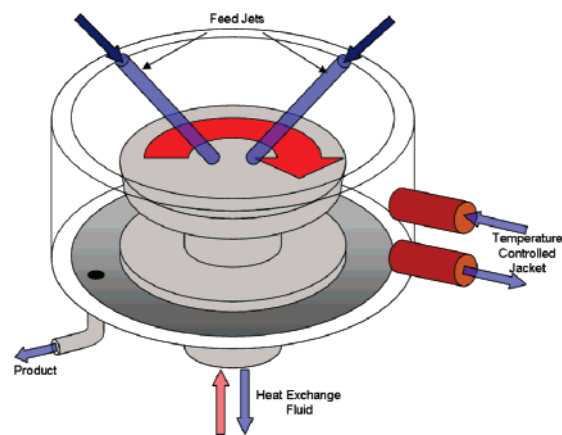


Figure 1. Schematic of a Spinning Disc Processor.

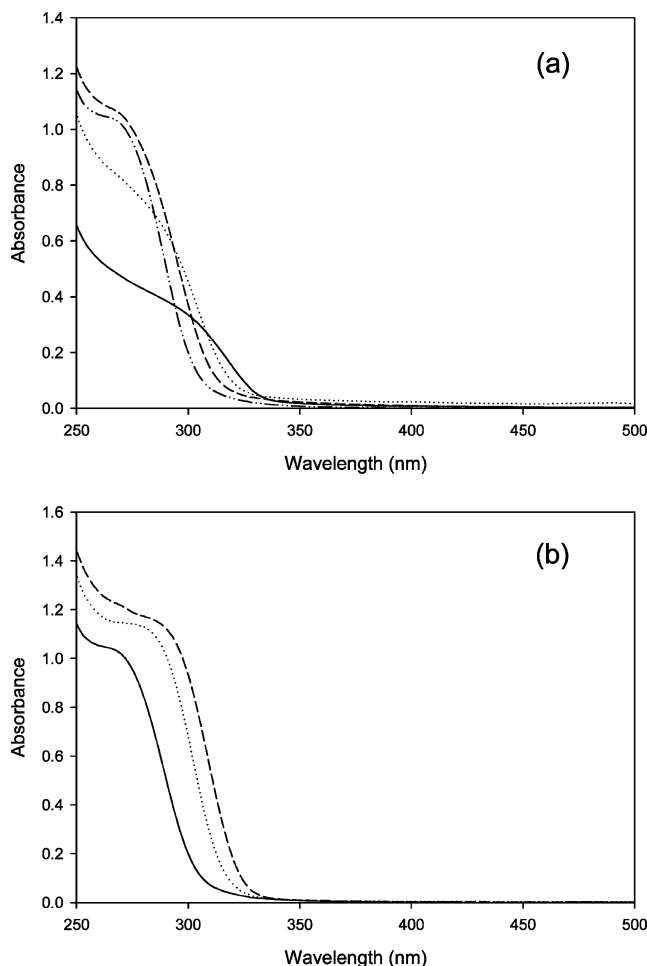


Figure 2. (a) Zn:NaOH:PVP10 1:1:0.05 wt % at 25 °C and: ---- 500 rpm, 1000 rpm, - · - · 2000 rpm, - · - · 3000 rpm. (b) Zn:NaOH:PVP10 1:1:0.05 wt % at 3000 rpm and: ---- 25 °C, 50 °C, - · - · 80 °C.

- (10) Izaki, M.; Mizuno, K.-T.; Shinagawa, T.; Inaba, M.; Tasaka, A. *J. Electrochem. Soc.* **2006**, *153*, C668–C672.
- (11) Lee, S. H.; Lee, S. S.; Choi, J.-J.; Jeon, J. U.; Ro, K. *Microsyst. Technol.* **2005**, 416–423.
- (12) Clarke, D. R. *J. Am. Ceram. Soc.* **1999**, 485–502.
- (13) Vayssieres, L.; Keis, K.; Lindquist, S.-E.; Hagfeldt, A. *J. Phys. Chem. B* **2001**, *105*, 3350–3352.
- (14) Spanhel, L. *J. Sol-Gel Sci. Technol.* **2006**, *39*, 7–24.
- (15) Sun, M.; Hao, W.; Wang, C.; Wang, T. *Chem. Phys. Lett.* **2007**, *443*, 342–346.
- (16) Li, M.; Hari-Bala; Lv, X.; Ma, X.; Sun, F.; Tang, L.; Wang, Z. *Mater. Lett.* **2007**, *61*, 690–693.
- (17) Guo, L.; Yang, S.; Yang, C.; Yu, P.; Wang, J.; Ge, W.; Wong, G. K. L. *Chem. Mater.* **2000**, *12*, 2268–2274.
- (18) Guo, L.; Yang, S.; Yang, C.; Yu, P.; Wang, J.; Ge, W.; Wong, G. K. L. *Appl. Phys. Lett.* **2000**, *76*, 2901–2903.
- (19) Nyffenegger, R. M.; Craft, B.; Shaaban, M.; Gorer, S.; Erley, G.; Penner, R. M. *Chem. Mater.* **1998**, *10*, 1120–1129.
- (20) Norberg, N. S.; Gamelin, D. R. *J. Phys. Chem. B* **2005**, *109*, 20810–20816.
- (21) Vergés, M. A.; Mifsud, A.; Serna, C. J. *J. Chem. Soc., Faraday Trans.* **1990**, *86*, 959–963.
- (22) Xiong, H.-M.; Liu, D.-P.; Xia, Y.-Y.; Chen, J.-S. *Chem. Mater.* **2005**, *17*, 3062–3064.
- (23) Liu, D.-P.; Li, G.-D.; Su, Y.; Chen, J.-S. *Angew. Chem., Int. Ed.* **2006**, *45*, 7370–7373.
- (24) Lee, W.; Jeong, M.-C.; Myoung, J.-M. *Acta Mater.* **2004**, *52*, 3949–3957.
- (25) Vanheusden, K.; Seager, C. H.; Warren, W. L.; Tallant, D. R.; Caruso, J.; Hampden-Smith, M. J.; Kodas, T. T. *J. Lumin.* **1997**, *75*, 11–16.
- (26) Amirav, L.; Amirav, A.; Lifshitz, E. *J. Phys. Chem. B* **2005**, *109*, 9857–9860.
- (27) Lamrani, M. A.; Addou, M.; Sofiani, Z.; Sahraoui, B.; Ebothé, J.; Hichou, A. E.; Fallahi, N.; Bernède, J. C.; Dounia, R. *Opt. Commun.* **2007**, *277*, 196–201.
- (28) Green Chemistry, <http://www.epa.gov/greenchemistry>.

commercial production, because these strategies are continuous flow processes; the tonnage generated is determined by the amount of time the processors are running. Process intensification is also highly compatible with the central themes of green chemistry.²⁹ The temperature of the disc and the surrounding jacket can be adjusted depending on the desired setup. This means that a fluid can be rapidly heated and cooled, and the very short residence time of fluid on the disc enables much higher reaction temperatures than

(29) Ramshaw, C. *Green Chem.* **1999**, *1*, G15–G17.

Table 1. Residence Times for Various Flow Rates and Disc Speeds at 25 °C

speed (rpm)	time (s)			
	1 mL/s	1.5 mL/s	2 mL/s	3 mL/s
500	0.55	0.42	0.35	0.27
1000	0.35	0.27	0.22	0.17
2000	0.22	0.17	0.14	0.1
3000	0.17	0.13	0.1	0.08

other conventional processors to be used. We have recently reported the use of SDP to control the particle size of β -carotene nanoparticles,³⁰ and the production of other particles has also been investigated.³¹ Another recent report has detailed the manufacture of metal nanoparticles under continuous flow with the ability to control particle size and size distribution by modification of particle average residence time.³²

Experimental Section

Materials. Zinc nitrate hexahydrate (98%, Asia Pacific Specialty Chemicals), sodium hydroxide (Redox Chemicals), potassium hydroxide (APS Ajax Fine Chemicals), polyvinylpyrrolidone (MW = 10000 g/mol, PVP10, Sigma-Aldrich), 27 wt % sodium silicate solution (Riedel-de Haën), and ethanol (CSR) were used as received. All reactions were performed on a spinning disc reactor (100 series, Protensive).

Synthesis. Under our experimental conditions, zinc nitrate hexahydrate is dissolved in ethanol along with 0.1 wt % polyvinylpyrrolidone. In a separate flask, the desired amount of base is dissolved in 100 mL of ethanol. These two solutions are then fed onto the surface of a 10 cm grooved or smooth spinning disc at a predetermined flow rate, where the temperature of the disc is set to 25, 50, or 80 °C and rotates at a speed of 500, 1000, 2000, or 3000 rpm.

Characterization. Transmission electron microscopy (TEM) was performed on a JEOL 2100 operating at an accelerating voltage of 120 kV and high-resolution TEM was performed on a JEOL 3000F operating at 300 kV. Samples for TEM were prepared by diluting the SDP product with ethanol in a ratio of product:ethanol = 1:4 and placing a 6 μ L drop onto a 200 mesh copper grid covered by a continuous amorphous carbon film. UV–visible spectroscopy was performed on a Perkin-Elmer Lambda 25 UV/vis spectrometer using matched quartz cuvettes with a path length of 1 cm and ethanol as the reference material. X-ray diffraction (XRD) was performed on a Siemens D5000 diffractometer.

Results and Discussion

Typical trends in UV–visible absorption are shown in Figure 2 for solutions that have come off the spinning disc processor immediately prior to the optical measurement. All results have been obtained using a flow rate of 1 mL/s and a grooved disc with grooves 0.65 mm apart and \sim 0.25 mm deep unless otherwise stated. It can clearly be seen that a disc speed of 500 rpm is insufficient to complete nucleation of ZnO nanoparticles, whereas the higher disc speeds all show very similar absorption features. This is likely due to the increased intensity of mixing that is achieved at higher

disc speeds, even though the residence time (time the fluid is exposed to high shear rates) is reduced. If we assume a synchronized flow model, where the liquid is rotating at the same speed as the disc, and the fluid flow is laminar, then shear stress, τ , and residence time, t , are given by the following equations³³

$$\tau = -1.5 \left(\frac{\eta \rho^2 Q r \omega^4}{18\pi} \right)^{1/3} \quad (1)$$

$$t = \left(\frac{81\pi^2 \eta}{16Q^2 \omega^2 \rho} \right)^{1/3} (r_0^{4/3} - r_i^{4/3}) \quad (2)$$

where Q is the volumetric flow rate, r is the disc radius, r_0 is the radius at exit from the disc, r_i is the radial distance of the feed inlet from the center of the disk, ω is the angular velocity of the disc, and η is the dynamic viscosity of the fluid. It is clearly seen that an increase in flow rate or disc speed will result in the generation of a larger shear stress, meaning more efficient mixing but a shorter residence time, and a larger disc will result in a larger average shear stress and longer residence time. Because these equations consider only laminar flow, they do not take into account an increase in mixing efficiency due to turbulent flow and therefore do not yield any information as to the effect of disc texture. It can be said, however, that a grooved disc will introduce more turbulence into the fluid flow than a smooth disc, and therefore, greater mixing efficiency can be achieved on a grooved disc. Table 1 shows residence times for various disc speeds and flow rates at 25 °C.

To determine the size and size distribution of the ZnO particles from the absorption spectra we have used the theoretical work of Sarma et al. and their subsequent least-squares fit.^{34–35} This method provides a quick and accurate assessment of size and polydispersity compared to conventional transmission electron microscopy methods. The theoretical model assumes that the polydispersity follows a Gaussian distribution function, which has previously been shown to reasonably approximate the true distribution.³⁵ The absorption edge and width have been determined from the first-order derivative of the absorption spectrum. There tends to be a decrease in particle size with increasing disc speed along with a decrease in the polydispersity of the particles produced as the speed of the disc is increased as seen in Figure 2a and Table 2. Size control is possible with variation in temperature and it is found that larger particles can be manufactured with increasing temperature as seen at 3000 rpm in Figure 2b. These results are easily reproduced, but all particles are found to undergo ripening at room temperature, which is commonly reported for many ZnO nanoparticle systems.^{36–39} Meulenkamp^{40,41} has also reported a least-

- (30) Anantchoke, N.; Makha, M.; Raston, C. L.; Reutrakul, V.; Smith, N. C.; Saunders, M. *J. Am. Chem. Soc.* **2006**, *128*, 13847–13853.
 (31) Cafiero, L. M.; Baffi, G.; Chianese, A.; Jachuck, R. J. *J. Ind. Eng. Chem. Res.* **2002**, *41*, 5240–5246.
 (32) Wu, C.; Zeng, T. *Chem. Mater.* **2007**, *19*, 123–125.

- (33) Oxley, P.; Brechtelsbauer, C.; Ricard, F.; Lewis, N.; Ramshaw, C. *Ind. Eng. Chem. Res.* **2000**, *39*, 2175–2182.
 (34) Viswanatha, R.; Sapra, S.; Satpati, B.; Satyam, P. V.; Dev, B. N.; Sarma, D. D. *J. Mater. Chem.* **2004**, *14*, 661–668.
 (35) Viswanatha, R.; Sarma, D. D. *Chem.—Eur. J.* **2006**, *12*, 180–186.
 (36) Koch, U.; Fojtik, A.; Weller, H.; Henglein, A. *Chem. Phys. Lett.* **1985**, *122*, 507–510.
 (37) Bahnmann, D. W.; Kormann, C.; Hoffmann, M. R. *J. Phys. Chem.* **1987**, *91*, 3789–3798.
 (38) Spanhel, L.; Anderson, M. A. *J. Am. Chem. Soc.* **1991**, *113*, 2826–2833.

Table 2. Size and Polydispersities for Zn:NaOH:PVP10 1:1:0.05 wt %

speed (rpm)	25 °C grooved disk		80 °C grooved disk		25 °C smooth disk	
	band gap (eV)	particle size (nm)	band gap (eV)	particle size (nm)	band gap (eV)	particle size (nm)
500	3.90	2.1 ± 16.2%	3.77	2.5 ± 19.6%	3.95	2 ± 16.9%
1000	4.09	1.75 ± 13.8%	4.00	1.9 ± 18.2%	4.20	1.6 ± 13%
2000	4.20	1.6 ± 13.8%	4.00	1.9 ± 13.5%	4.34	1.45 ± 10.9%
3000	4.29	1.5 ± 11%	4.00	1.9 ± 12.6%	4.46	1.3 ± 10%

squares fit of the relationship between particle size and band gap from experimental data. Although this particular approach considered only particle sizes between 2.5 and 6.5 nm, we found that this method gave results consistent with the theoretical model, e.g., for particles with an average diameter of 1.5 nm using the approach discussed by Sarma et al.,³⁴ Meulenkamp's approach (using his fit of all data)⁴⁰ gives 1.8 nm. These data are also consistent with particle sizing data from Mulvaney et al.³⁹

XRD particle sizing has also been employed as a complementary technique to confirm the data from optical measurements. Particle size was determined from the width of the diffraction peak at $2\theta \sim 47.4^\circ$ using the Scherrer equation.¹⁸ XRD gives results consistent with the optical data. For example, for Zn:NaOH:PVP10 1:1:0.05 wt % at 25 °C and 3000 rpm, XRD gives an average particle size of 1.4 nm with an associated measurement error of ± 0.2 nm (see the Supporting Information), compared to Sarma et al.'s approach, which gives 1.5 nm. We therefore believe that the optical technique provides a quick and reliable assessment of particle size. To overcome the problem of ripening, samples were immediately cooled with liquid nitrogen post-SDP, and a 2.7 wt % aqueous solution of sodium silicate was then added under intense stirring. The sample was then stored at 2 °C overnight prior to rotary evaporation and washing with water.

Nucleation has been reported to be an activation-controlled process,^{37,39} but Figure 2a clearly shows that variation of SDP parameters, other than temperature, strongly influences the rate of nucleation. Temperature also influences the amount of ZnO formed off the spinning disc with greater UV-vis absorption intensity observed at higher temperatures for all speeds. This increase is significantly larger at lower disc speeds. Because there appears to be a correlation between shear stress (mixing efficiency) and nucleation, it could be implied that a diffusion-controlled nucleation process is occurring on the surface of the disc. Other possibilities include the occurrence of localized heat analogous to cavitation in ultrasonic mixing or that another usable form of energy other than heat is being transferred to the reaction mixture to allow an activation-controlled process to occur.

Selected area electron diffraction by TEM of an aged sample shows that the sample is crystalline ZnO in the standard wurtzite structure (Figure 3a).⁴² The wurtzite structure is confirmed by XRD. Diffraction rings corresponding to the $\{101\}$ and $\{102\}$ planes for wurtzite ZnO are absent in the selected area diffraction pattern. Upon careful examination of high-resolution images (for example, Figure 3b), it can be seen that the majority of the particles lie down either the $\langle 001 \rangle$ or $\langle 101 \rangle$ zone axis, so it is likely that the effect seen in the electron diffraction pattern is due to preferred orientation, potentially a result of the presence of faceted or platelike particles; this could mean that ripening occurs along specific crystallographic directions.

The effect of the base and concentration of base that is used can clearly be seen in Figure 4. For NaOH and KOH, much more nucleation is achieved at Zn²⁺:OH⁻ ratios of 1:2 than at 1:1, but NaOH appears to be a more effective base at lower temperatures for nucleation and growth of ZnO compared to KOH, which is clearly seen in a comparison

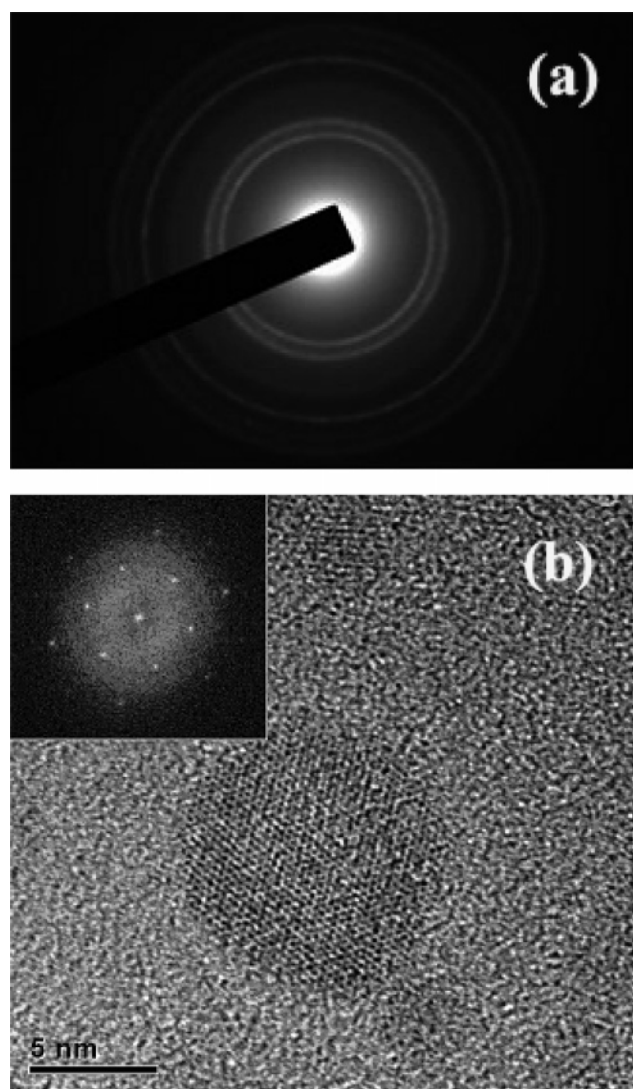


Figure 3. (a) Selected area diffraction pattern and (b) high-resolution TEM image of aged ZnO nanoparticles prepared using Zn:KOH:PVP10 1:2:0.05 wt % at 25 °C and 2000 rpm (Inset: Fourier transform of central particle).

(39) Wood, A.; Giersig, M.; Hilgendorff, M.; Vilas-Campos, A.; Liz-Marzán, L.; Mulvaney, P. *Aust. J. Chem.* **2003**, *56*, 1051–1057.

(40) Meulenkamp, E. A. *J. Phys. Chem. B* **1998**, *102*, 5566–5572.

(41) Meulenkamp, E. A. *J. Phys. Chem. B* **1998**, *102*, 7764–7769.

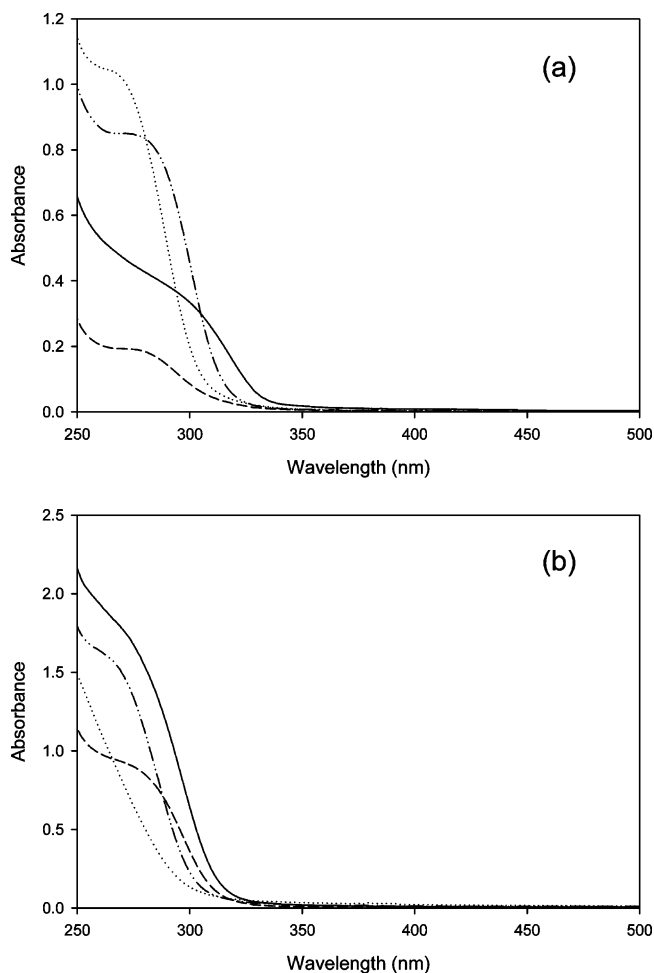


Figure 4. Effect of base and base concentration at 25 °C and 0.05 wt % PVP: (a) --- Zn:NaOH = 1:1, 500 rpm; Zn:NaOH = 1:1, 3000 rpm; --- Zn:KOH = 1:1, 500 rpm; --- Zn:KOH = 1:1, 3000 rpm. (b) --- Zn:NaOH = 1:2, 500 rpm; Zn:NaOH = 1:2, 3000 rpm; --- Zn:KOH = 1:2, 500 rpm; --- Zn:KOH = 1:2, 3000 rpm.

between absorption intensities for NaOH and KOH under similar SDP conditions. Also, a small amount of a fine white ZnO precipitate is observed after aging for 1 h at room temperature for both NaOH and KOH at a $\text{Zn}^{2+}:\text{OH}^-$ ratio of 1:2, indicating excessive growth of ZnO. At 25 °C and 1:2 $\text{Zn}^{2+}:\text{NaOH}$, the absorption spectrum for 500 rpm shows a typical absorption feature for ZnO at 296 nm and the absorption edge blue shifts with increasing disc speed until 2000 rpm. At 3000 rpm, the absorption spectrum does not show the characteristic absorption edge for ZnO but there is an absorption onset at ~ 295 nm that is similar to other UV-vis absorption spectra of very small particles.³⁷ Therefore, by comparison with other results, it is unlikely that the lack of an absorption band at 3000 rpm is due to little or no reaction taking place, and we believe therefore that non-luminescent, subnanometer clusters have formed that show absorption features masked by the OH^- charge transfer solvent band at ~ 210 nm.³⁹ The use of KOH at $\text{Zn}^{2+}:\text{OH}^- = 1:2$ and 25 °C gives larger particles than those synthesized with NaOH.

Differences in ripening behavior between ZnO synthesized with NaOH and KOH are also observed. For all disc speeds

and temperatures, it is found that for samples prepared with NaOH there is a red-shift of the absorption edge with time. A decrease in absorption intensity is also observed, which is typically observed during particle ripening.³⁹ However, for a disc speed of 500 rpm, no significant change in absorption intensity is observed. For samples prepared with KOH, a red-shift of the absorption edge is also observed with time; however, this is associated with a large increase in absorption intensity. This increase is indicative of significantly more ZnO being produced after the reactants have been subjected to SDP. At 500 rpm, this is followed by a slow decline of absorption intensity with a further red-shift of the absorption edge, indicating further ripening (see the Supporting Information). No initial increase in absorption intensity is observed, indicating that no more ZnO is formed in the presence of NaOH post-SDP for a disc speed of 500 rpm. As the reaction is not complete off the disc at 500 rpm, it is unclear at this stage why the two bases give different outcomes, although it may be related to differences in the ability of the metal cation to passivate the surface of the nanoparticle.⁴³

As the temperature of the disc is increased for the $\text{Zn}^{2+}:\text{OH}^- = 1:2$ systems, we find that for NaOH only 500 rpm at 50 °C gives a stable, colorless solution. At higher disc speeds and temperatures, the product solution is turbid and a white precipitate rapidly forms at the bottom of the collection vial; consequently, no UV-vis data could be obtained. This was not observed for KOH with stable, colorless solutions obtained over the entire range of disc speeds and temperatures. For both bases and $\text{Zn}^{2+}:\text{OH}^-$ ratios, it was found that as the temperature increases the particle size and polydispersity also increase, which appears to be consistent with other literature.^{37,39} This work and the work of others suggest that synthesis of small ZnO nanoparticles is better achieved at lower temperatures, so we would expect that cooling the disc would provide small and highly monodisperse ZnO particles so long as nucleation is completed on the surface of the disc, but this is beyond the current SDP capability. The colloidal solutions could then be kept at low temperature and passivated more effectively (e.g., with an inorganic shell) to hinder particle ripening. The use of anhydrous conditions may also provide a better environment for the formation ZnO, because it has been noted that water is deleterious for the formation of small ZnO nanoparticles.³⁹

If the flow rate of the reagent solutions is increased to 2 mL/s total (2×1 mL/s) for $\text{Zn}^{2+}:\text{NaOH} = 1:1$ at 25 °C, we find that the absorption spectrum is red-shifted and more intense than a 1 mL/s flow rate, as seen in Figure 5. If the flow rate is further increased to 3 mL/s total (2×1.5 mL/s) then a blue-shift compared to the 1 mL/s data is observed for the 500 rpm system with an associated increase in absorption intensity. At 3000 rpm and 3 mL/s, a broad absorption feature is observed with a much lower intensity, indicating that much less nucleation has occurred using these SDP parameters. We believe these phenomena are caused by interplay between surface shear rate and fluid residence

(42) Note: TEM analysis was not used for unaged material as the sample contains a large amount of polymer, which was impossible to remove without some degree of ripening occurring.

(43) Viswanatha, R.; Amenitsch, H.; Sarma, D. D. *J. Am. Chem. Soc.* **2007**, *129*, 4470–4475.

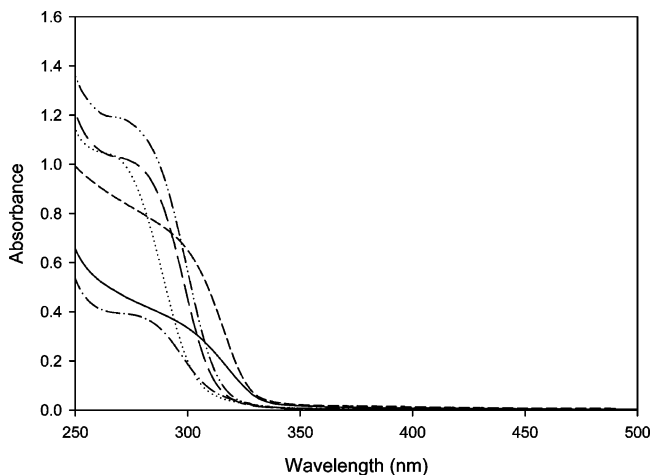


Figure 5. Effect of flow rate for Zn:NaOH:PVP10 1:1:0.05 wt % at 25 °C: --- 500 rpm, 1 mL/s; 3000 rpm, 1 mL/s; --- 500 rpm, 2 mL/s; --- 3000 rpm, 2 mL/s; --- 00 rpm, 3 mL/s; -·-·- 3000 rpm, 3 mL/s.

time on the disc surface. At 2 mL/s, there is an increased surface shear rate that leads to a greater intensity of mixing, which seems to cause a greater rate of nucleation and growth. At 3 mL/s, for 1000 rpm and above, the absorption intensities drop because even though there is a larger surface shear rate, there is insufficient time for nucleation to complete on the surface of the disc. A flow rate of 3 mL/s, however, seems to be the best flow rate tested for a 500 rpm disc speed, because it provides the most intense absorption spectrum compared to all other tested flow rate regimes.

The use of different flow rates for the two feeds combined with changes to the reagent concentrations provides another mechanism for investigating the effects of flow rate while maintaining a constant mole ratio of $\text{Zn}^{2+}:\text{OH}^-$. In all systems that feed the zinc/PVP source at double the rate of the base feed, in conjunction with doubling the concentration of base, a higher absorption intensity than the corresponding system at equal flow rates of Zn^{2+} /PVP and base is observed. For NaOH, this is also associated with a particle size increase seen by the red-shift in the absorption edge. This is again a consequence of the faster rate of nucleation and growth observed for NaOH over KOH as well as the higher overall concentration of ZnO present in the product. When the feed concentrations are adjusted so that the concentration of the product equals that for 1:1 flow rate systems at 500 rpm, the absorption spectrum is slightly blue-shifted with equal intensity. At disc speeds greater than 1000 rpm, there is no characteristic absorption edge for ZnO present, which is again indicative of the formation of subnanometer clusters. Interestingly, under this flow rate regime, the difference between 25 and 50 °C is marginal, which differs from the results obtained using equal flow rates (shown in Figure 2b).

Another parameter that can be modified is the surface texture of the disc. The surface texture modifies the mixing characteristics of the fluids and can therefore influence the reaction rate and growth of ZnO nanoparticles. If the grooved disc is replaced with a smooth disc of the same diameter, then it is generally found that the absorption intensity is lower than that of the same system prepared using a grooved disc for a Zn:OH⁻ ratio of 1:1, Figure 6. This is expected because

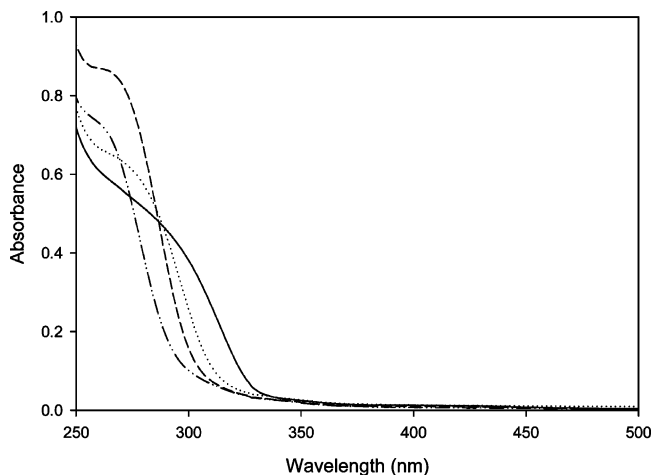


Figure 6. Absorption spectra of products using smooth disc texture for Zn:NaOH:PVP10 = 1:1:0.05 wt % at 25 °C: --- 500 rpm, 1000 rpm, --- 2000 rpm, -·-·- 3000 rpm.

the mixing intensity that can be achieved using the smooth disc is far less than the grooved disc. Interestingly, however, for $\text{Zn}^{2+}:\text{OH}^- = 1:2$ at 25 °C using NaOH and KOH, the absorption spectra for ZnO nanoparticles produced using the smooth disc are very similar to those produced using the grooved disc. This may be a result of the rate of nucleation being controlled mainly by the concentration of base rather than the turbulence in the fluid created by the spinning disc. At 50 °C, using NaOH, the smooth disc gives a transparent solution with no precipitate at all disc speeds, which is in stark contrast to the product obtained on the grooved disc at the same temperature. In fact, temperature appears to have far less influence when the smooth disc is used at the temperatures tested. Another feature of the smooth disc is that at $\text{Zn}^{2+}:\text{NaOH} = 1:1$, the influence of disc speed is enhanced, and at faster disc speeds, the absorption edge is blue-shifted. Also, the onset of absorption is red-shifted, as seen in the tail on the absorption spectrum, which again is a result of the slower rate of nucleation with the smooth disc. When the flow rate is increased using a smooth disc, we see that the absorption spectrum is now blue-shifted but a tail is still present and the changes in absorption intensity are similar to those for the grooved disc.

The only SDP parameters that have not been altered in this investigation are disc diameter and wall temperature. An increase in the disc diameter will increase the time the fluid is exposed to conditions of intense mixing, which, from the results presented here, may lead to larger particles and/or a more intense UV-vis absorption spectrum. A larger disc may also be useful for promoting nucleation in slower reactions. The temperature of the walls can also have an influence on the final particle size. Heating of the walls may promote ripening while cooling could quench ripening.

Conclusion

In summary, small, monodisperse ZnO nanoparticles can be produced under continuous flow conditions using spinning disc processing. SDP gives control over the synthetic conditions and allows for the reliable reproduction of ZnO nanoparticles under specific SDP parameters. It is generally found that an increase in shear stress as a result of either an

increase in disc speed and/or flow rate, or modification of the surface texture enhances the rate of nucleation on the surface of the disc. Very small nanoparticles can be obtained from SDP, and the particle size and polydispersity is found to increase with an increase in disc temperature. Further investigation of disc texture and temperature may yield greater insight into the process, as it has been shown that disc texture modifies the rate of nucleation and it is likely that with a further reduction of temperature smaller polydispersities could be realized. This methodology could also be applied to the synthesis of many other semiconducting nanomaterials, potentially on a commercial scale.

Acknowledgment. The work was supported by the Australian Research Council (ARC) and The University of Western Australia Fledgling Centre Program (UWA-FCP). TEM work was carried out using facilities at the Centre for Microscopy, Characterisation and Analysis, The University of Western Australia, which are supported by University, State, and Federal Government funding. K.J.H. acknowledges the award of a Hackett Postgraduate Scholarship from UWA.

Supporting Information Available: XRD data of fresh and ripened samples and UV–vis absorption spectra displaying ripening behavior (PDF). This material is available free of charge via the Internet at <http://pubs.acs.org>.

CM0715646